

# A Single Amino Acid Limits the Substrate Specificity of *Thermus thermophilus* Uridine-Cytidine Kinase to Cytidine

Fumiaki Tomoike,<sup>‡</sup> Noriko Nakagawa,<sup>§,||</sup> Seiki Kuramitsu,<sup>‡,§,||</sup> and Ryoji Masui<sup>\*,§,||</sup>

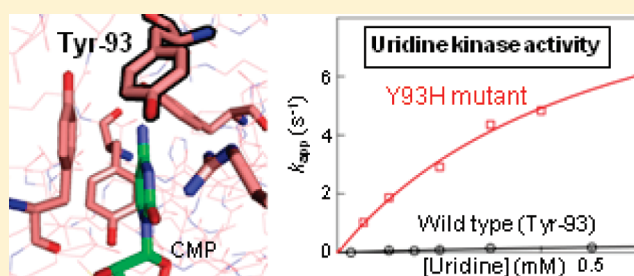
<sup>‡</sup>Graduate School of Frontier Biosciences, Osaka University, 1-3 Yamadaoka, Suita, Osaka 565-0871, Japan

<sup>§</sup>Department of Biological Sciences, Graduate School of Science, Osaka University, 1-1 Machikaneyama-cho, Toyonaka Osaka 560-0043, Japan

<sup>||</sup>RIKEN SPring-8 Center, 1-1-1 Kouto, Sayo-cho, Sayo-gun, Hyogo 679-5148, Japan

 Supporting Information

**ABSTRACT:** The salvage pathways of nucleotide biosynthesis are more diverse and are less well understood as compared with de novo pathways. Uridine-cytidine kinase (UCK) is the rate-limiting enzyme in the pyrimidine-nucleotide salvage pathway. In this study, we have characterized a UCK homologue of *Thermus thermophilus* HB8 (ttCK) biochemically and structurally. Unlike other UCKs, ttCK had substrate specificity toward only cytidine and showed no inhibition by UTP, suggesting uridine does not bind to ttCK as substrate. Structural analysis revealed that the histidine residue located near the functional group at position 4 of cytidine or uridine in most UCKs is substituted with tyrosine, Tyr93, in ttCK. Replacement of Tyr93 by histidine or glutamine endowed ttCK with phosphorylation activity toward uridine. These results suggested that a single amino acid residue, Tyr93, gives cytidine-limited specificity to ttCK. However, replacement of Tyr93 by Phe or Leu did not change the substrate specificity of ttCK. Therefore, we conclude that a residue at this position is essential for the recognition of uridine by UCK. In addition, thymidine phosphorylase from *T. thermophilus* HB8 was equally active with thymidine and uridine, which indicates that this protein is the sole enzyme metabolizing uridine in *T. Thermophilus* HB8. On the basis of these results, we discuss the pyrimidine-salvage pathway in *T. thermophilus* HB8.



Nucleoside triphosphates (NTPs) are essential for all living organisms because NTP acts as an energy source and a component of essential molecules including DNA, RNA, and coenzymes. In de novo pathways, nucleotides are synthesized from low molecular weight precursor molecules. The de novo pathway requires a relatively large amount of energy: for example, the synthesis of purine nucleotide requires at least six high-energy bonds per molecule of purine produced.<sup>1</sup> Therefore, organisms also recycle degradation products such as bases and nucleosides through salvage pathways.

There are two salvage pathways for ribonucleotides: one is for free bases and the other is for ribonucleosides (Figure 1).<sup>2,3</sup> In the first salvage pathway for pyrimidine nucleotides, uracil is converted to UMP through the direct transfer of sugar phosphate by uracil phosphoribosyltransferase (EC 2.4.2.9). Cytosine is recycled through the same pathway after deamination to uracil by cytosine deaminase (EC 3.5.4.1). Uracil can be produced from uridine by uridine phosphorylase (EC 2.4.2.3) or thymidine phosphorylase (EC 2.4.2.4). For recycling cytidine in this pathway, cytidine must be converted to uridine by cytidine deaminase (EC 3.5.4.5). In the second pathway, the ribonucleosides, uridine and cytidine, are directly transformed to their monophosphate form, UMP and CMP, by further phosphorylation catalyzed by uridine-cytidine

kinase (UCK) (EC 2.7.1.48). UCK is the rate-limiting enzyme in the pyrimidine-nucleotide salvage pathway.<sup>4</sup> UCK has been reported to be highly expressed in rapidly dividing cells.<sup>5,6</sup> CMP and UMP produced by UCK are subsequently phosphorylated by nucleotide kinases to form NTPs.

The salvage pathways of nucleotide biosynthesis are more diverse and are less well understood. Recent developments in comparative genomics suggest that there is still much to learn about the diversity of microbial enzymes involved in the metabolism of nucleotides. Figure 1 shows the ratio of species that have the indicated enzymes in the (selected) 191 bacterial species whose genome sequences have been determined. The enzymes mentioned above are not conserved in all species. Even UCK is found in only half of the 191 species. In addition, novel enzymes and pathways for nucleotide metabolism have been found. For example, characterization of a phosphofructokinase-family protein has revealed a novel nucleoside kinase.<sup>7</sup> These findings suggest that respective organisms have different pathways composed of varying combinations of enzymes. In addition, a few

**Received:** December 24, 2010

**Revised:** March 26, 2011

**Published:** May 03, 2011

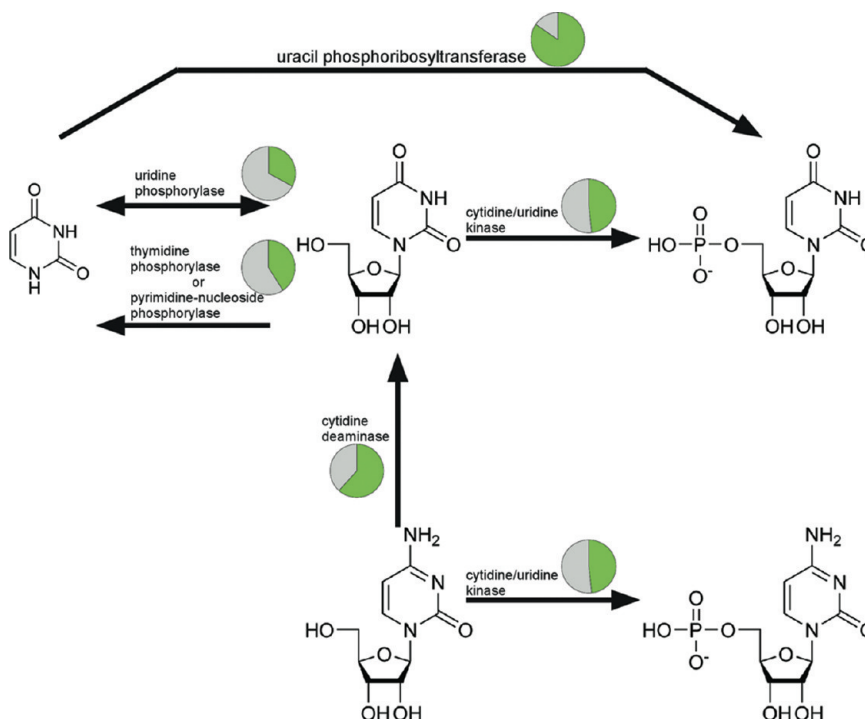


**Figure 1.** Pyrimidine nucleoside metabolism pathways for uridine. Pie charts indicate the ratio of bacterial species (green, from a total of 191 species) that use the described enzyme (NCBI genome project page <http://www.ncbi.nlm.nih.gov/genomeprj>).

substitutions of amino-acid residues in active site can change substrate specificity of nucleoside kinases.<sup>8–10</sup> Therefore, it is important in the detailed study of a nucleotide salvage pathway to target a single organism.

In this study, we characterized the UCK homologue of *T. thermophilus* HB8 (ttCK) biochemically and structurally. Because proteins from this extremely thermophilic eubacterium are stable and most genes have been cloned in the whole cell project,<sup>11</sup> the enzymes from this organism are highly suitable for biochemical studies. Although UCK is an important enzyme that catalyzes the rate-limiting step, tertiary structure of UCK has been reported only for human UCK,<sup>12,13</sup> and mechanism of substrate specificity in UCK has not been investigated in detail. Our kinetic study revealed that ttCK has the substrate specificity toward only cytidine. To our knowledge, there have been no reports about a UCK family protein with cytidine-specific activity; thus, ttCK has the novel substrate specificity. We determined the X-ray crystal structure of ttCK in complex with CMP, which is the first reported structure of a prokaryotic UCK. We found one amino acid substitution among the conserved residues comprising the active site. Mutational analysis indicated that the cytidine-limited specificity of ttCK can be attributed to a single amino-acid residue. In addition, our study suggests that thymidine phosphorylase of *T. thermophilus* HB8 (ttTP) is active toward uridine, as well as thymidine. On the basis of these results, we propose probable salvage pathways for pyrimidine nucleotides in *T. thermophilus* HB8.

## MATERIALS AND METHODS

**Protein Overexpression and Purification.** ttCK (ORF ID, TTHA0578) and ttTP (TTHA1771) expression plasmids (obtained from RIKEN BioResource Center) were transformed into *Escherichia coli* Rosetta(DE3). The transformants were

cultured at 37 °C in 1.5 L of LB medium supplemented with 50  $\mu\text{g mL}^{-1}$  of ampicillin for 23 h. Cells were harvested by centrifugation. ttCK was purified by heat treatment at 60 °C for 20 min and column chromatography with a Toyopearl SP-650 column (Tosoh) and Superdex 200 10/300 GL column (GE Healthcare Biosciences). For purifying ttTP, a Toyopearl SuperQ-650 column (Tosoh), Toyopearl Butyl-650 column (Tosoh), and Superdex 75 10/300 GL column (GE Healthcare Biosciences) were used after heat treatment at 65 °C for 20 min. The concentrations of the purified proteins were determined by using molar absorption coefficients, calculated to be 11 200 and 26 600  $\text{M}^{-1} \text{cm}^{-1}$  at 278 nm for ttCK and ttTP, respectively.<sup>14</sup>

**Physicochemical Measurements.** To determine the apparent molecular mass, purified ttCK (50  $\mu\text{M}$ ) was applied to a Superdex 75 10/300 GL column at a flow rate of 0.5  $\text{mL min}^{-1}$ . The apparent molecular weight was estimated by comparing its retention time with those of molecular weight markers containing  $\beta$ -amylase from sweet potato (200 000 Da), alcohol dehydrogenase from yeast (150 000 Da), albumin from bovine serum (66 000 Da), and carbonic anhydrase from bovine erythrocytes (29 000 Da) (Sigma).

The circular dichroism (CD) spectrum in the far-UV region from 200 to 250 nm was obtained at 25 °C with a Jasco spectropolarimeter, J-720W, using 1.2  $\mu\text{M}$  ttCK in 20 mM Tris-HCl at pH 7.5. Thermostability was investigated by recording the molar ellipticity at 222 nm from 25 to 95 °C at pH 7.5.

**Enzyme Assay of ttCK.** To screen for nucleoside specificity, the reaction mixture contained 20 mM Tris-HCl, 100 mM KCl, 10 mM divalent cation, 50  $\mu\text{M}$  each nucleoside (adenosine, guanosine, uridine, cytidine, deoxyadenosine, deoxyguanosine, thymidine, and deoxycytidine), 550  $\mu\text{M}$  (d)NTP, and 50 nM ttCK at pH 8.0. To screen for (d)NTP specificity, ATP, GTP, CTP, UTP, ITP, dATP, or dGTP was used. To screen for divalent cation specificity,  $\text{MgCl}_2$ ,  $\text{CaCl}_2$ , or  $\text{ZnCl}_2$  was used. The reaction

mixtures were incubated at 25 or 70 °C for 1 h. Reaction product analyses were performed by ion-pair chromatography<sup>15</sup> with some modifications. In these experiments, a CAPCELL PAK C18 column (Shiseido) was used for separation of nucleosides and nucleotides. The  $k_{\text{cat}}$  and  $K_M$  values of ttCK and its mutants for cytidine were determined by using an NADH-dependent enzyme-coupled assay<sup>16</sup> with a Hitachi UV spectrophotometer, U-3000. Measurements were performed at 25 °C in solutions containing 20 mM HEPES (pH 7.2), 100 mM KCl, 20 mM MgCl<sub>2</sub>, 50–300  $\mu$ M cytidine, 2 mM (for WT), or 300  $\mu$ M (for mutants) ATP, 15  $\mu$ M NADH, 15  $\mu$ M phosphoenolpyruvate, 0.5 mU of lactate dehydrogenase from pig heart (Toyobo), 0.5 mU of pyruvate kinase from rabbit muscle (Sigma), and 0.5  $\mu$ M ttCK. For the measurements of inhibition, the concentrations of UTP and CTP were 0–100  $\mu$ M and 0–2  $\mu$ M, respectively.

**Enzyme Assay of ttTP.** Reaction mixtures contained 20 mM potassium phosphate (pH 7.5), 100 mM KCl, 500  $\mu$ M uridine or thymidine, and 25 nM ttTP. Reactions were performed at 25 °C for 5 min. The reaction was stopped by adding 100 mM trichloroacetic acid to a final concentration of 25 mM. The reaction products were analyzed with a CAPCELL PAK C18 column at a flow rate of 1.0 mL min<sup>−1</sup>. The mobile phase was 0.25–30% methanol in 10 mM potassium phosphate buffer (pH 7.8). The rate constants for the phosphorolysis reactions were calculated by measuring the decrease in absorbance at 260 nm. In this measurement, reaction mixtures contained 20 mM HEPES (pH 7.2), 100 mM KCl, 20 mM potassium phosphate, 350 nM ttTP, and 5–50  $\mu$ M uridine or 5–75  $\mu$ M thymidine. Reactions were initiated by adding ttTP.

**Crystallization, Data Collection, and Structure Determination.** Crystals of the ligand-free ttCK and the ttCK-CMP complex were obtained in a solution of 67% No. 34 (40% (v/v) isopropanol, 15% (w/v) PEG 8000, and 0.1 M imidazole, pH 6.5) from Precipitant Synergy Screen (Emerald Biosystems) and 33% distilled water, and a solution of 100% No. 27 (50% (w/v) PEG 200 and 0.1 M Tris-HCl, pH 8.0) from Cryo II screen set (Emerald Biosystems), respectively, using the 96-well sitting-drop vapor-diffusion method at 20 °C.<sup>17</sup> A 0.5  $\mu$ L aliquot of the crystallization reagent was mixed with 0.5  $\mu$ L of 25 mg mL<sup>−1</sup> protein solution. This mixture was covered with 15  $\mu$ L of a silicone and paraffin oil solution. For crystallization of the ttCK-CMP complex, the protein solution contained 1 mM CMP, 1 mM ADP, and 1 mM MgCl<sub>2</sub>. Data were collected with the RIKEN Structural Genomics Beamline II (BL26B2)<sup>18</sup> at SPring-8 (Hyogo, Japan). Data were processed by using the HKL-2000 program suite.<sup>19</sup> Structures were solved by using a molecular replacement method with Molrep.<sup>20</sup> The coordinates of human uridine-cytidine kinase 2 (PDB code 1UEJ)<sup>12</sup> were used as the starting model. Model refinement was carried out by using the programs Xtalview<sup>21</sup> and CNS.<sup>22</sup> According to PROCHECK,<sup>23</sup> the final models of ttCK without and with CMP have 85.2% and 91.5%, respectively, of their residues in the most favored region of the Ramachandran plot, and no residues were found in the forbidden regions for either structure. The data-collection statistics and processed data statistics are presented in Table 1. Crystallographic coordinates for the two structures [ttCK (3ASY) and ttCK-CMP complex (3ASZ)] have been deposited in the PDB.

**Site-Directed Mutagenesis.** Site-directed mutagenesis of ttCK was performed by using the method of Iwai et al.<sup>24</sup> with some modifications. Overexpression and purification of the mutant protein were performed in a manner similar to that used for wild type (WT).

**Table 1. Data Collection and Refinement Statistics for ttCK and Its Complex with CMP<sup>c</sup>**

data set	free	CMP–ttCK complex
Crystal parameters		
space group	P43212	P21212
unit-cell parameters (Å)		
<i>a</i>	70.364	68.7300
<i>b</i>	70.364	126.9420
<i>c</i>	179.243	61.000
Data processing		
resolution (Å)	50–2.40	50–2.25
no. of measured reflections	2141,379	723,725
completeness (%)	100 (100)	100.0 (100.0)
Redundancy	12.9 (13.7)	9.5 (8.9)
<i>I</i> / $\sigma$ ( <i>I</i> )	53.7 (8.3)	39.8 (7.4)
<i>R</i> <sub>merge</sub> (%) <sup>a</sup>	6.4 (35.2)	10.5 (30.0)
Refinement parameters		
resolution range ( <i>F</i> > 0) (Å)	50.0–2.4	50.0–2.25
no. of reflection	15,903	26,274
<i>R</i> <sup>b</sup>	0.2330	0.1990
<i>R</i> <sub>free</sub>	0.2995	0.2407
no. of atoms		
protein	3180	3269
water	90	194
ligand	0	42
average <i>B</i> value (Å <sup>2</sup> )	27.6	35.1
r.m.s.d.		
bond lengths (Å)	0.009	0.009
bond angles (°)	1.451	1.728

<sup>a</sup>  $R_{\text{merge}} = \sum_{hkl} \sum_i |I_i(hkl) - \langle I(hkl) \rangle| / \sum_{hkl} \sum_i I_i(hkl)$ , where  $\langle I(hkl) \rangle$  is the average of individual  $I_i(hkl)$  measurements. <sup>b</sup>  $R = \|F_o\| - \|F_c\| / \|F_o\|$ .

<sup>c</sup> Values in parentheses are for the outermost shell.

## RESULTS

**Physicochemical Properties of ttCK.** ttCK gene (TTHA0578) encodes a protein of 222 amino acid residues with a calculated molecular mass of 23 674 Da and a theoretical pI of 9.3. The recombinant ttCK was purified to homogeneity from *E. coli* by three steps of chromatography after heat treatment. Size exclusion chromatography indicated that the apparent molecular mass of ttCK was 66 kDa (data not shown), which suggested that ttCK forms a dimer or trimer in solution. The far-UV CD spectrum of ttCK had negative double maxima at about 210 and 225 nm (data not shown), suggesting that ttCK contains  $\alpha$ -helical structures. The temperature dependence of the ellipticity at 222 nm indicated that ttCK was stable up to approximately 70 °C at pH 7.0 (data not shown).

**Enzyme Activity of ttCK.** We first examined the substrate specificity of ttCK activity using ion-pair chromatography. This method can directly quantify nucleotides and nucleosides separately (Figure 2). The reaction mixture contained eight nucleosides as candidates for acceptors of phosphate from ATP. After incubation at 25 °C for 1 h, ATP was consumed while ADP was produced (Figure 2A). With regard to the phosphate acceptor, cytidine was consumed and CMP was produced concomitantly. However, the amounts of other nucleosides including uridine and deoxycytidine were not changed (Figure 2B,C), indicating

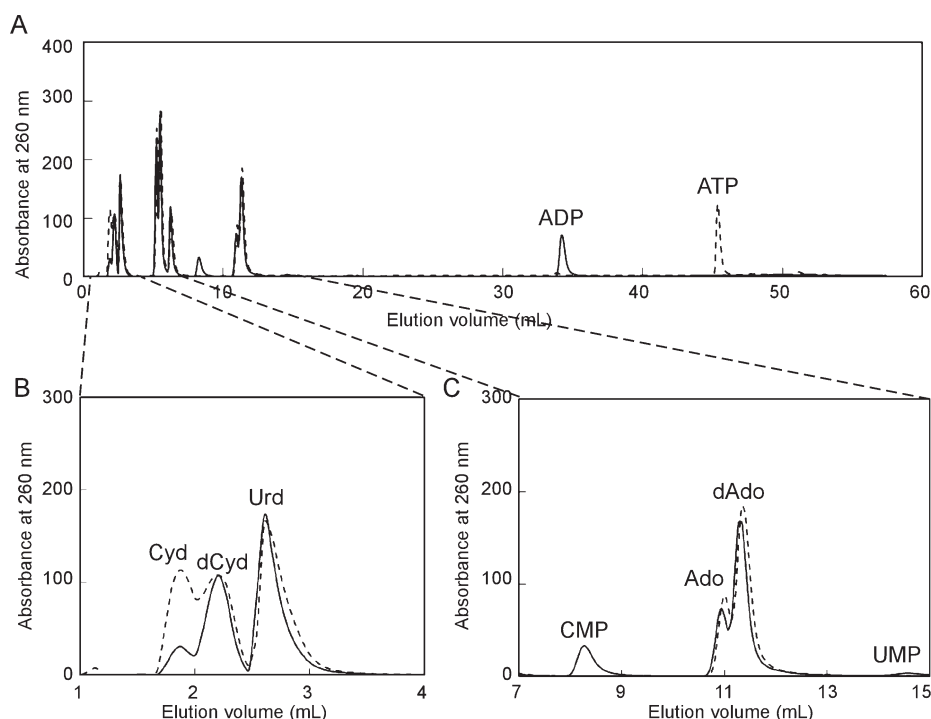


**Figure 2.** Substrate specificity of ttCK. (A) Ion-pair chromatography of the reaction products after incubation of ttCK with eight nucleosides and ATP. Reactions were performed with ttCK (solid line) or without ttCK (broken line). (B and C) Expansions of (A) showing the cytidine and uridine peaks and CMP and UMP peaks, respectively.

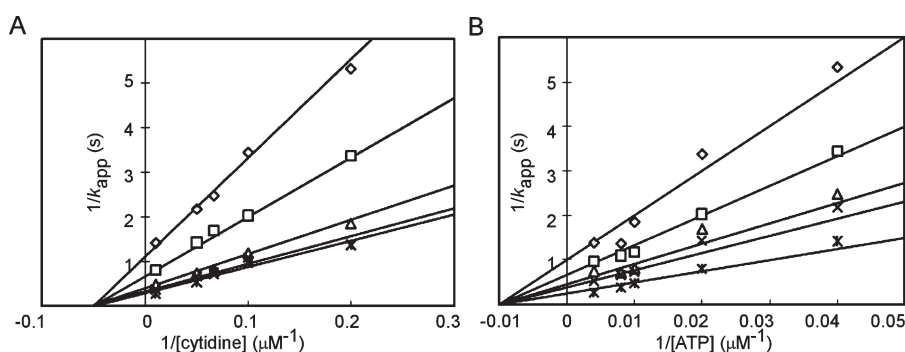


**Figure 3.** Double reciprocal plots of  $1/k_{app}$  versus  $1/[cytidine]$  (A) and  $1/[ATP]$  (B). (A) The concentrations of ATP were 25  $\mu M$  (diamonds), 50  $\mu M$  (squares), 100  $\mu M$  (triangles), 125  $\mu M$  (crosses), and 250  $\mu M$  (asterisks). (B) Concentrations of cytidine were 5  $\mu M$  (diamonds), 10  $\mu M$  (squares), 15  $\mu M$  (triangles), 20  $\mu M$  (crosses), and 100  $\mu M$  (asterisks).

that no other nucleoside was converted to its corresponding nucleoside monophosphate. NTPs (GTP, UTP, or ITP) or dNTP (dATP or dGTP) as well as ATP worked for the phosphorylation of cytidine (data not shown). Even when  $Mg^{2+}$  was replaced by another divalent cation ( $Ca^{2+}$  or  $Zn^{2+}$ ), ttCK catalyzed the phosphorylation of only cytidine (data not shown). It should be noted, however, that when CTP was used as the phosphate donor, even cytidine was not phosphorylated. This result suggested that cytidine phosphorylation catalyzed by ttCK is inhibited competitively by CTP, a feature that has been reported on UCKs (this will be examined later).<sup>12,25</sup> Reactions at 70 °C also had no effect on this high specificity toward cytidine (data not shown). These results demonstrated that ttCK phosphorylates only cytidine. Because UCK family proteins have been reported to phosphorylate both cytidine and uridine in previous

reports,<sup>4,25,26</sup> we concluded that ttCK has a cytidine-limited specificity.

To elucidate the reaction mechanism of ttCK, the initial velocity of cytidine phosphorylation by ttCK was measured at various concentrations of cytidine and ATP. Figure 3A,B shows double reciprocal plots of  $1/k_{app}$  versus  $1/[cytidine]$  and  $1/[ATP]$ , respectively, at 20 mM  $MgCl_2$ . Even at 1 mM  $MgCl_2$ , a concentration close to the free magnesium concentration in *T. thermophilus* HB8 cells,<sup>27</sup> similar results were obtained (data not shown). The  $k_{cat}$  values were constant under various concentrations of  $MgCl_2$  (Figure S1, Supporting Information). The  $k_{cat}$  and  $K_M$  values of ttCK for cytidine were 4.1  $s^{-1}$  and 72  $\mu M$ , respectively, under the concentration of ATP at which the activity of ttCK was the highest (Table 2). These values were similar to those of known UCKs.<sup>26,28</sup> The initial velocity of bisubstrate



**Table 2. Kinetic Parameters of WT and Mutant ttCK<sup>a</sup>**

enzyme	substrate	$k_{\text{cat}}$ (s <sup>-1</sup> )	$K_{\text{M}}$ (μM)	$k_{\text{cat}}/K_{\text{M}}$ (M <sup>-1</sup> s <sup>-1</sup> )	$K_{\text{I}}^{\text{CTP}}$ (μM)	$K_{\text{I}}^{\text{UTP}}$ (μM)
WT	cytidine	4.1 ± 0.8	72 ± 24	5.7 × 10 <sup>4</sup>	6.0 ± 0.4	n. d.
	uridine	n. d.	n. d.	n. d.		
Y59F	cytidine	6.4 ± 2.5	200 ± 68	3.2 × 10 <sup>4</sup>		
	uridine	n. d.	n. d.	n. d.		
Y93H	cytidine	8.4 ± 1.1	220 ± 27	3.8 × 10 <sup>4</sup>	7.3 ± 0.6	720 ± 240
	uridine	9.2 ± 1.7	360 ± 43	2.6 × 10 <sup>4</sup>		
Y93F	cytidine	5.9 ± 1.7	100 ± 49	5.7 × 10 <sup>4</sup>		
	uridine	n. d.	n. d.	1.2 × 10 <sup>-2</sup>		
Y93L	cytidine	10 ± 4	420 ± 11	2.4 × 10 <sup>4</sup>		
	uridine	n. d.	n. d.	6.6 × 10 <sup>-3</sup>		
Y93Q	cytidine	2.8 ± 0.5	230 ± 33	1.2 × 10 <sup>4</sup>		
	uridine	1.1 ± 0.4	1,600 ± 590	7.2 × 10 <sup>2</sup>		

<sup>a</sup> n. d.: not detected.

enzyme reactions can be fitted to eqs 1 and 2 below, which show the sequential mechanism and the ping-pong mechanism, respectively, of bisubstrate reaction.<sup>29</sup>

$$v = k_{\text{cat}}[E][A][B]/(K_{\text{ia}}K_{\text{b}} + K_{\text{a}}[B] + K_{\text{b}}[A]) \quad (1)$$

$$v = k_{\text{cat}}[E][A][B]/(K_{\text{a}}[B] + K_{\text{b}}[A] + [A][B]) \quad (2)$$

In these equations,  $K_{\text{a}}$  and  $K_{\text{b}}$  are Michaelis constants for substrate A and B, respectively, and  $K_{\text{ia}}$  is the diffusion constant of substrate A. If an enzymatic reaction goes through a ping-pong mechanism, we will get a parallel pattern in the double-reciprocal plot. If it goes through a sequential mechanism, we will get an intersecting pattern. When the cytidine concentration was varied against different concentrations of ATP, the double reciprocal plots of the initial velocity were intersecting lines rather than parallel lines, and vice versa (Figure 3A,B). These results indicated that the reaction mechanism of ttCK is sequential. This feature agrees with those of other UCKs.<sup>30</sup> From the double reciprocal plots of the apparent  $k_{\text{cat}}$  values versus the substrate concentration (Figure S2, Supporting Information), we determined the turnover numbers at infinite concentrations of respective substrate.

**The Crystal Structure of ttCK.** To elucidate the reason for the exclusion of uridine by ttCK, the crystal structures of ttCK without and with CMP were determined at resolutions of 2.40 Å and 2.25 Å, respectively (Figure 4). To our knowledge, this is the first report describing a prokaryotic UCK structure. The overall structure is highly similar to that of human uridine cytidine kinase 2 (human UCK2).<sup>12</sup> The crystal structure of human UCK1 has also been resolved (PDB ID, 2JEO and 2UVQ), but has not yet been published. In the ttCK crystals, the asymmetric unit contained two ttCK molecules. Furthermore, two dimers of ttCK can be related by a crystallographic symmetry operation, suggesting that ttCK exists as a tetramer in the crystal lattice. The tetrameric state is similar to that of human UCK2.<sup>12</sup> The total buried surface area of 610 Å<sup>2</sup> also reflected a true dimer interface.

Each subunit is comprised of nine α-helices and seven β-strands, among which a four-stranded β-sheet is sandwiched between four α-helices (Figure 4A). Owing to their poor electron density, the terminal regions (residues 1–4 and 204–211) of the ligand-free form were not built into the model. The two ttCK molecules in the asymmetric unit are nearly isomorphous in both

the ligand-free form (rmsd = 0.53 Å) and the CMP-bound form (rmsd = 0.39 Å).

Comparison of the ligand-free structure and the CMP-ttCK complex structure indicated that substrate binding induces a significant conformational change (Figure 4B). CMP is bound to both ttCK molecules in the asymmetric unit. The conformations of the two CMP molecules are almost identical. Upon binding of CMP, the substrate-binding cavity closes: the distance between the Cα atoms of Phe90 and Arg150 changes from approximately 13.1 Å to 4.8 Å (Figure 4B).

In the ttCK-CMP complex structure, hydrogen bonds are formed between ttCK and CMP (Figure 4C). The cytosine base of the bound CMP molecule makes hydrogen bonds with the side chains of Tyr88, Arg152, and Gln160. The ribose group forms hydrogen bonds with Asp60 and Arg142. These two residues are thought to play an important role in distinguishing between ribose and deoxyribose because they interact with the 2' oxygen atom of the ribose moiety. The nonbridging oxygen atoms of the phosphate group interact with the side chains of Thr15, Lys19, Arg145, and Arg150. These interacting residues are highly conserved among UCK family members. In addition, Tyr59 and Tyr93 are located near the base of CMP (Figure 5A). The distances between the cytosine and Tyr59 and Tyr93 are 4.9 and 5.1 Å, respectively, which seem too far for direct interactions. However, these residues are located near the N4 amino group and the N3 nitrogen atom of cytosine, atoms that differ between cytosine and uracil. Therefore, these residues are considered to be key residues conferring the cytidine-limited specificity of ttCK.

In order to identify the main residue conferring the cytidine-limited specificity, we compared the structures of the nucleoside-binding site between ttCK-CMP and human UCK2-cytidine complex (Figure 5A,B). We found that most amino acid residues around the base moieties are identical between ttCK and human UCK2, except for Tyr59 and Tyr93 in ttCK (corresponding to Phe83 and His117 in human UCK2). Sequence comparison of ttCK and other UCK family proteins showed that the residue equivalent to Phe83 in human UCK is tyrosine in many organisms, including *E. coli* and *T. thermophilus* HB8 (Figure 5C). This observation suggested that Tyr59 does not play a critical role in cytidine specificity, thus leaving Tyr93 as the likely candidate. Many UCK homologues, including human UCK1 and *E. coli* UCK has a histidine residue at the position equivalent to Tyr93 in ttCK.

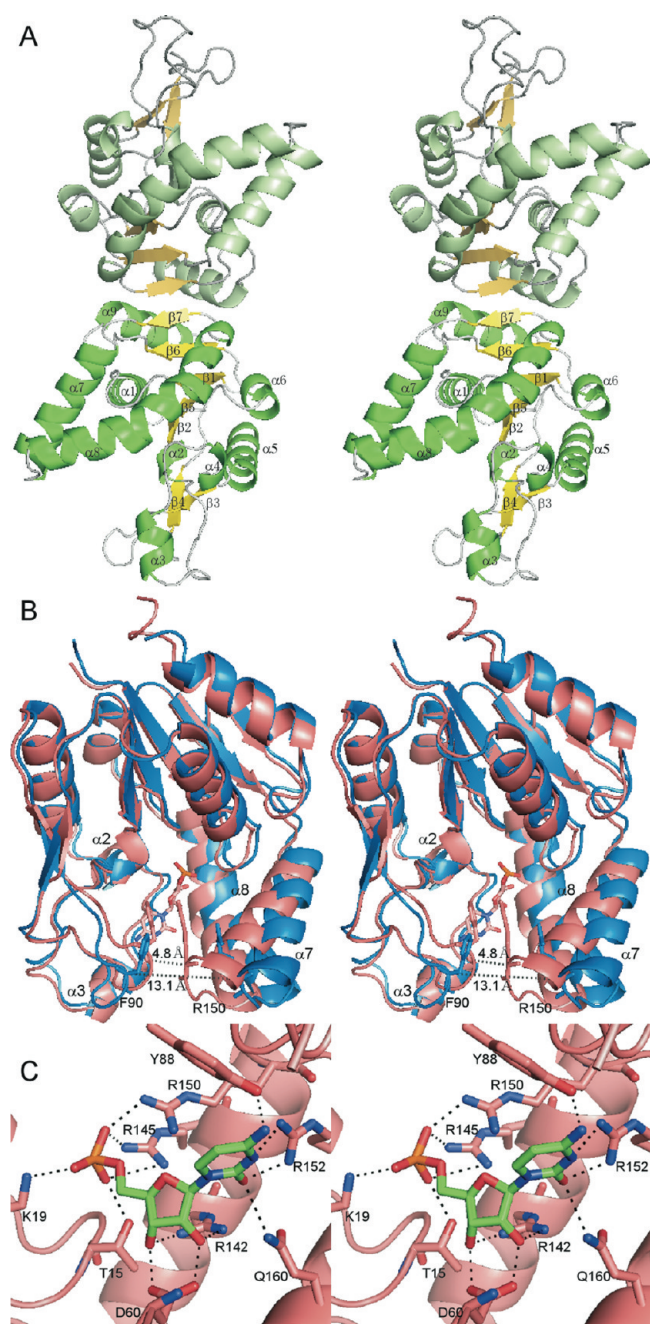


**Figure 4.** Stereo diagram of the ttCK crystal structure. (A) Secondary structure of the ttCK dimer. (B) Comparison of the ttCK monomer in the presence (red) and the absence (blue) of CMP. Binding of CMP reduced the distance between the C $\alpha$  atoms of Phe90 and Arg150 by approximately 8 Å. (C) The interaction between CMP and ttCK. The ttCK residues that interact with CMP and CMP itself are shown as sticks models in stereo. The cartoon model of ttCK and carbon atoms in the stick model and CMP are shown in red and green, respectively. Dot lines represent hydrogen bonds.

**Enzyme Activity of Tyr59 and Tyr93 Mutants.** In order to assess the contribution of Tyr59 and Tyr93 to the limited substrate specificity of ttCK, we prepared two ttCK mutants, Y59F and Y93H, in which the amino acid substitution was modeled on human UCK2. The activity of WT and these mutants toward cytidine and uridine was measured by using an NADH-dependent

enzyme coupled assay (Figure 6). The kinetic constants are shown in Table 2. The substrate specificity of Y59F was the same as that for WT. In contrast, Y93H had activity for both uridine and cytidine. The  $k_{\text{cat}}/K_M$  values of Y93H for these two nucleosides were similar, indicating that Y93H has substantial activity toward uridine as well as cytidine. This result suggests that Tyr93 contributes to the substrate specificity of ttCK.

In order to evaluate the contribution of the functional group of Tyr93 to substrate binding, we generated three other Tyr93 mutants and determined their kinetic constants. Because a tyrosine residue contains one hydroxyl group and one phenyl group, we replaced Tyr93 with a phenylalanine residue (Y93F) and a leucine residue (Y93L) to test the contribution of the hydroxyl and phenyl group, respectively. In addition, we replaced Tyr93 with a glutamine residue (Y93Q) for evaluating whether the activity of Y93H for both uridine and cytidine is linked to the ability of a histidine residue to serve as both hydrogen acceptor and donor. With respect to uridine, the Y93F and Y93L mutants showed faint activity, which was too small to calculate the individual  $K_M$  and  $k_{\text{cat}}$  values, and thus only the  $k_{\text{cat}}/K_M$  values were determined (Table 2). The result indicated that both mutants had deficient activity toward uridine. With respect to cytidine, the  $k_{\text{cat}}$  values of the Y93F and Y93L mutants were equivalent to that of WT, indicating that these mutations had no significant effect on catalytic activity. On the other hand, the  $K_M$  value of Y93L for cytidine was significantly higher (6-fold) than that of WT. The finding implied that a smaller residue at this position provides a higher  $K_M$  value for cytidine. Meanwhile, Y93Q had the activity toward both uridine and cytidine (Table 2). The uridine phosphorylation activity of Y93Q was strikingly higher than that of WT, Y93F, and Y93L. The  $K_M$  and  $k_{\text{cat}}$  values of Y93Q for uridine were higher (4.5-fold) and lower (9-fold) than those of Y93H, respectively.

**Enzyme Inhibition by CTP and UTP.** We then examined whether UTP and CTP inhibited the activity of WT and Y93H. It is known that CTP and UTP inhibit UCK family proteins competitively by binding to the nucleoside-binding site, demonstrating a feedback system that inhibits and regulates the pyrimidine ribonucleoside salvage pathway.<sup>4</sup> We measured the activity of ttCK toward cytidine in the presence of various concentration of UTP or CTP. Double-reciprocal plots indicated that CTP inhibited the activity of both WT and Y93H competitively, but UTP inhibited only Y93H and not WT (Figure 7). The inhibition constants ( $K_i$ ) of WT and Y93H for CTP were much smaller than the respective  $K_M$  values for cytidine (Table 2). The  $K_i$  value of Y93H for UTP was larger than that for CTP by an order of magnitude but still smaller than the  $K_M$  value for cytidine (Table 2). These results indicated that Tyr93 prevents UTP from binding to the nucleoside-binding site in ttCK. Therefore, we concluded that the uridine-binding deficiency of ttCK results in weak activity toward uridine.

**Enzyme Activity of ttTP.** The cytidine-specific activity of ttCK prompted the question of how uridine is metabolized in *T. thermophilus* cells. General salvage pathways of pyrimidine nucleosides are known (Figure 1). The genome annotation predicted that *T. thermophilus* HB8 has a gene (TTHA0735) encoding cytidine deaminase, which produces uridine from cytidine. In addition to the route involving UCK, uridine can be converted into uracil by uridine phosphorylase, and then uracil can be converted into UMP by uracil phosphoribosyltransferase. The gene annotation of the *T. thermophilus* HB8 genome predicted the presence of a uracil phosphoribosyltransferase (TTHA1312), but not a uridine phosphorylase. However, some



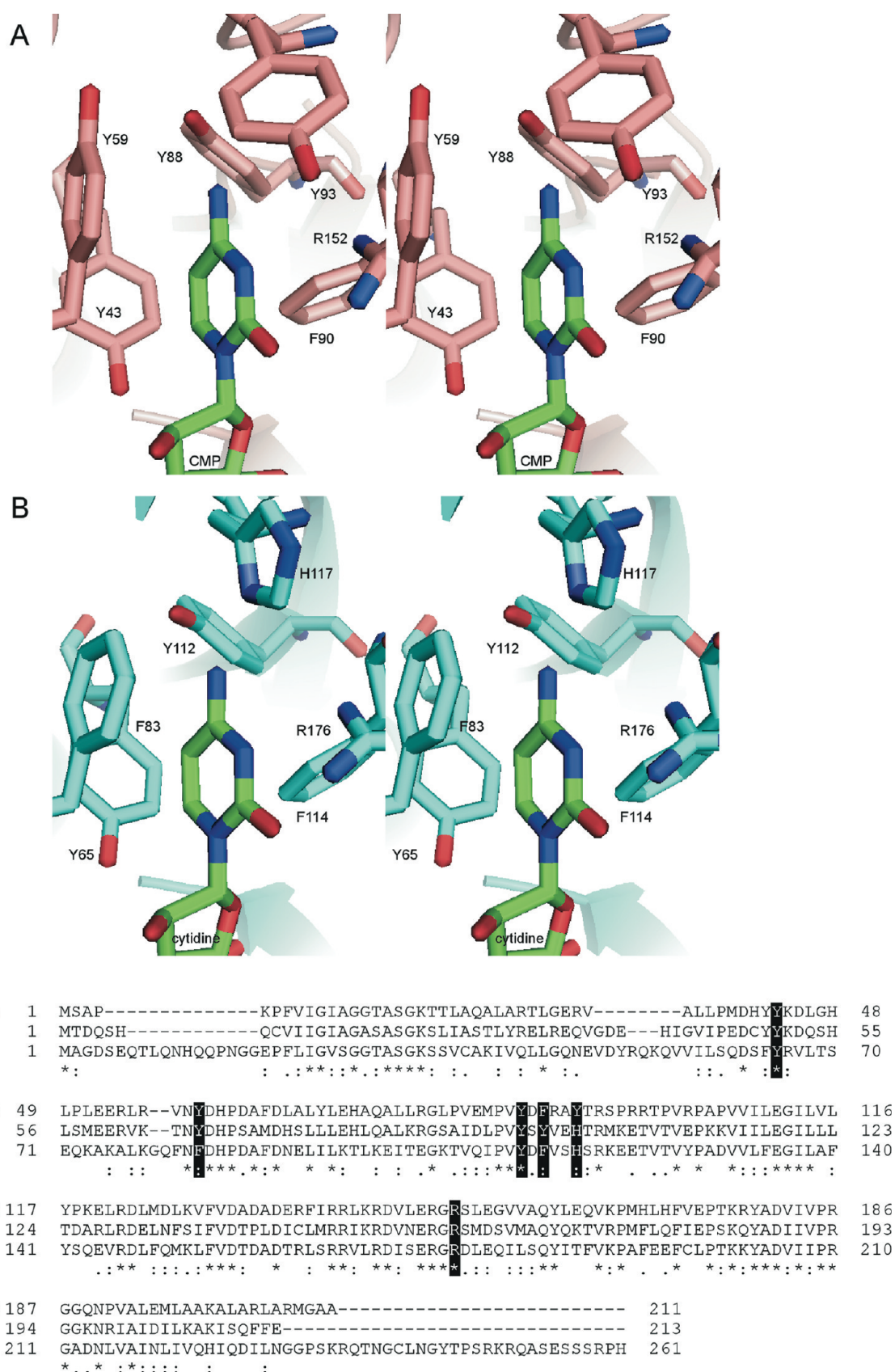


**Figure 5.** Comparison of ttCK and its homologues. (A and B) Stereo diagrams of ttCK and human UCK2, respectively. (C) The sequence comparison of ttCK and UCK family proteins from *E. coli* and human. It has been reported that UCK family proteins from *E. coli* and human have activity toward cytidine and uridine.

thymidine phosphorylases have activity toward uridine as well as thymidine,<sup>31,32</sup> and *T. thermophilus* HB8 has a gene (TTHA1771) encoding thymidine phosphorylase. This observation raised the possibility that TTHA1771 (ttTP) has uridine phosphorylase activity in addition to thymidine phosphorylase activity.

In order to examine the substrate specificity of ttTP, we purified ttTP as a recombinant protein and assayed its phosphorylase activity by HPLC analysis. The results showed that ttTP catalyzes the conversion of thymidine and uridine to thymine and uracil, respectively (Figure 8A). By quantitative spectroscopic analysis, we found that ttTP exhibits higher activity toward uridine than thymidine (Figure 8B and Table 3). Therefore, these findings suggested that uridine can be converted into uracil by ttTP in *T. thermophilus* HB8 cells.

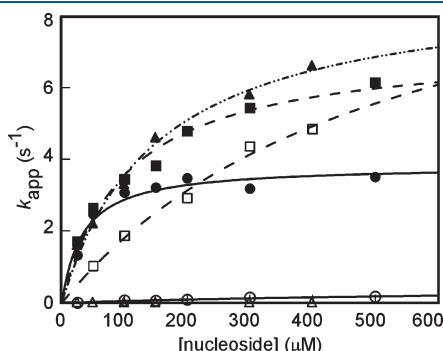


**Figure 6.** Activity of WT ttCK and mutants toward uridine and cytidine. The activities of ttCK WT, (circles), Y59F (triangles), and Y93H (squares) were measured by an NADH-dependent enzyme coupled assay. The substrate was uridine (open symbols) or cytidine (filled symbols). The data for WT, Y59F, and Y93H are fitted with solid, dot-dash, and broken lines, respectively.

## DISCUSSION

**Mechanism Underlying Nucleoside Specificity.** This study showed that ttCK has activity toward only cytidine, making it the first report of a cytidine-specific UCK from any organism. The mutational studies indicated that Tyr93 (or the residue at position 93) contributes to the specificity of nucleoside binding (Table 2). Only when Tyr93 was replaced with histidine or glutamine, uridine

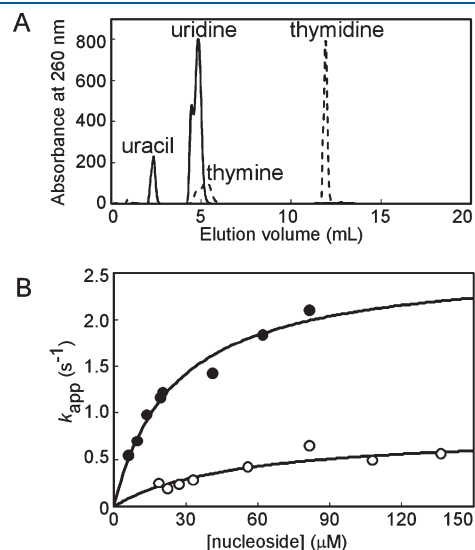


**Figure 8.** Phosphorylase activity of ttTP. (A) Products of the ttTP-catalyzed reaction with uridine or thymidine. The reactions were performed with uridine (solid line) or thymidine (broken line). (B) Initial velocities of ttTP. The initial velocities were measured at various concentrations of uridine (filled circles) or thymidine (open circles). The solid lines are computer-fitted theoretical curves.

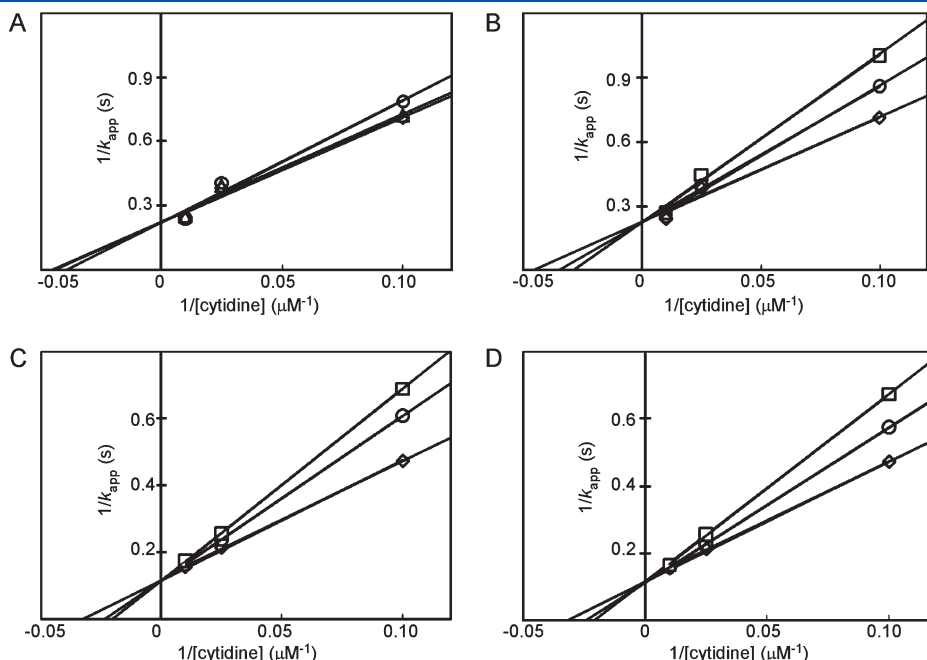


**Figure 7.** Inhibition of the cytidine kinase activity of WT (A and B) and Y93H (C and D) ttCK by UTP or CTP. The results are shown as double reciprocal plots. The concentrations of the inhibitors were 0  $\mu$ M, 50  $\mu$ M, and 100  $\mu$ M UTP (A), 0  $\mu$ M, 1  $\mu$ M, and 2  $\mu$ M CTP (B), 0  $\mu$ M, 20  $\mu$ M, and 40  $\mu$ M UTP (C), and 0  $\mu$ M, 1  $\mu$ M, and 2  $\mu$ M CTP (D). The concentrations of inhibitor in each panel are indicated in descending order as squares, circles, and diamonds.



**Table 3. The Activity of ttTP**

substrate	$k_{\text{cat}}$ ( $\text{s}^{-1}$ )	$K_{\text{M}}$ ( $\mu\text{M}$ )	$k_{\text{cat}}/K_{\text{M}}$ ( $\text{M}^{-1} \text{s}^{-1}$ )
uridine	$2.6 \pm 0.8$	$16 \pm 10$	$1.0 \times 10^5$
thymidine	$0.9 \pm 0.3$	$45 \pm 19$	$2.2 \times 10^4$

phosphorylation activity was detected (Figure 6 and Table 2). When Tyr93 was replaced with a smaller residue (Phe or Leu), significant activity toward uridine could not be detected. In addition, inhibition analysis suggested that uridine could not bind to ttCK (Table 2). These results indicate that the histidine residue at this position is the determinant of uridine binding of UCK. In other words, it can be said that the tyrosine residue (in the wild-type ttCK), as well as phenylalanine and leucine residues at this position, cannot accept uridine as a nucleoside substrate.

It can be reasonably presumed that the functional group at position 4 is critical for discrimination between cytidine and uridine by UCK. We first expected that tyrosine excluded uridine. Unexpectedly, however, phenylalanine and leucine at this position also excluded uridine. These findings suggest that the OH group and the bulky phenyl group of tyrosine hardly contribute to such substrate discrimination. Phosphorylation of uridine by Y93H mutant supports the notion that bulkiness of the side chain is not a critical factor. The size of an amino group is larger than that of a keto group, which could enable an enzyme to exclude cytidine. In fact, however, ttCK excluded uridine but not cytidine. This finding also seems to dismiss the notion that a difference in the size of the side chains contributes to substrate discrimination. Because histidine and glutamine could accept uridine, it is reasonable to suppose that the amine group at this position permits a uridine-specific interaction.

The structural study showed that the distance between Tyr93 and the 4-amino group of CMP is too far for a direct interaction (Figure 5). Although we have not elucidated the structure of the cytidine-bound complex, the structure determined might reflect a binding step of the substrate because cytidine and CMP (as well as CTP and UTP) bind similarly to the nucleoside-binding site in human UCK2.<sup>12</sup> In the case of human UCK2, His117 and Tyr112 are thought to form hydrogen bonds with the functional groups of the respective bases.<sup>12</sup> Our structure might reflect a “pre-binding” step of the substrate.

From the viewpoint of functionality, both amino and keto groups can form a hydrogen bond, but only the latter can be a hydrogen acceptor. Thus, it is possible to postulate a keto-group-specific interaction with a particular hydrogen donor. Indeed, His117 forms a hydrogen bond with the keto group of bound UTP in the human UCK2 structure.<sup>12</sup> In that case, the O4 atom of uridine forms a hydrogen bond with the protonated N $\delta$ 1 atom of His117. If the N $\delta$ 1 atom of His117 is protonated, it cannot be expected to form a hydrogen bond with the N4 atom of cytidine. This seems to meet the requirement for the keto-group-specific interaction. It should be mentioned, however, that Suzuki et al have suggested that there is a hydrogen bond between His117 and the amino group of cytidine: in that case, the N $\delta$ 1 atom is deprotonated and the hydrogen atom is provided by the cytidine. Direct identification of the position of the hydrogen atom is required for clarification of this point. The observation that Y93Q had uridine phosphorylation activity also supports the notion that a keto group of uridine specifically interacts with a particular hydrogen donor.

Our mutational analysis together with the above hypothesis suggests that the histidine at position 93 is dispensable for the activity toward cytidine. In ttCK, substitution of histidine for tyrosine at this position caused increased  $K_{\text{M}}$  value for cytidine (Table 2). The  $K_{\text{M}}$  value of Y93F was similar to that of WT, whereas Y93L had increased  $K_{\text{M}}$  value, implying that bulkiness of the side chain makes some contribution to the activity toward cytidine. To verify whether the histidine at this position is also dispensable for cytidine recognition in other UCKs, mutational analysis of His117 of human UCK2 should be carried out. Tyr59 is considered to be involved in the recognition of cytidine by ttCK because the Y59F mutant had increased  $K_{\text{M}}$  value reduced affinity. Although human UCK2 has a phenylalanine residue at this position, many organisms have a tyrosine residue at this position. Y59F showed no activity toward uridine.

**Physiological Implication for Uridine Metabolism.** We found that ttCK was unable to metabolize uridine but that ttTP had activity toward uridine (Figure 8). ttTP was originally annotated as thymidine phosphorylase, but it also functioned as a uridine phosphorylase. Interestingly, ttTP exhibited higher catalytic activity for uridine than for thymidine. ttTP did not phosphorylate cytidine like other thymidine phosphorylases (data not shown). Thus, this enzyme (TTHA1771) should be designated as a pyrimidine-nucleoside phosphorylase [EC 2.4.2.2], rather than a thymidine phosphorylase [EC 2.4.2.4]. The X-ray crystal structure of ttTP has been determined by the structural genomics project (PDB ID, 2DSJ), but not been published as yet.

Because there is no paralogue of ttCK in the *T. thermophilus* HB8 genome, ttTP can be considered to be the sole enzyme metabolizing uridine in *T. thermophilus* HB8. This metabolism might contribute to maintain the concentration of UTP and CTP. The intracellular concentration of UTP is approximately 100  $\mu\text{M}$  and is equal to that of CTP.<sup>33</sup> Unlike human UCK2, the cytidine kinase activity of ttCK is inhibited by CTP, but not UTP (Figure 7). Thus, even when the concentration of UTP is higher than CTP, cytidine could be phosphorylated by ttCK and recycled to CTP independently of UTP. Conversely, when the concentration of CTP is increased, CTP could inhibit ttCK, leading to increased conversion of cytidine to uridine by cytidine deaminase (Figure 1). As a result, uridine would be converted to UTP via uracil. As compared with pathway involving usual UCKs, such a salvage metabolism is simpler but well organized. This metabolic network may provide benefits to an organism regardless of the GC content of its genome.

In addition to ttCK, other UCK homologues have tyrosine at the position equivalent to Tyr93. Such enzymes, which are found in several species such as *Lactobacillus reuteri*, *Listeria monocytogenes*, and *Mycoplasma pneumonia* among others, are predicted to be cytidine-specific UCKs (Figure S3, Supporting Information). These putative cytidine-specific UCKs are distributed in at least 15 different genera, and are not restricted to a particular group of bacteria. This may suggest an ancient origin of this type of UCK.

Detailed studies on nucleoside metabolism have the potential to inform several areas of clinical research, including the development of nucleoside analogues for antiparasitic and antiviral drugs, as well as the chemotherapy of cancer. Some organisms, typically parasitic organisms, cannot synthesize nucleotides de novo. Insight into the structure and mechanism of the enzymes involved can aid in the development of potent inhibitors. This study points to the critical need for experimental studies even of enzymes whose annotation has been accepted.

## ■ ASSOCIATED CONTENT

**S Supporting Information.** A figure of  $k_{\text{cat}}$  values of ttCK under various  $\text{MgCl}_2$  concentrations, plots of  $k_{\text{cat}}$  dependence on ATP and cytidine concentrations, and a figure of sequence alignment of putative cytidine-specific UCK. This material is available free of charge via the Internet at <http://pubs.acs.org>.

## Accession Codes

Coordinates have been deposited as Protein Data Bank (PDB) entries 3ASY and 3ASZ.

## ■ AUTHOR INFORMATION

### Corresponding Author

\*Telephone: +81-6-6850-5434. Fax: +81-6-6850-5442. E-mail: [rmasui@bio.sci.osaka-u.ac.jp](mailto:rmasui@bio.sci.osaka-u.ac.jp).

## ■ ACKNOWLEDGMENT

We thank Yumiko Inoue for her help in purification of ttCK. We also thank Toshi Arima for her help in crystallization, and Yuka Nonaka for her help in data collection at SPring-8.

## ■ ABBREVIATIONS USED

NTP, nucleoside triphosphate; NDP, nucleoside diphosphate; UCK, uridine-cytidine kinase; ttCK, UCK (TTHA0578) from *T. thermophilus* HB8; tTP, thymidine phosphorylase (TTHA1771) from *T. thermophilus* HB8; WT, wild type; CD, circular dichroism

## ■ REFERENCES

- (1) Voet, D., Voet, J. G., and Pratt, C. W. (2008) *Principles of Biochemistry*, 3rd ed., international student version, pp 817–847, Wiley, New York.
- (2) O'Donovan, G., and Neuhaud, J. (1970) Pyrimidine metabolism in microorganisms. *Bacteriol. Rev.* 34, 278–343.
- (3) Turnbough, C. L. J., and Switzer, R. L. (2008) Regulation of pyrimidine biosynthetic gene expression in bacteria: repression without repressors. *Microbiol. Mol. Biol. Rev.* 72, 266–300.
- (4) Anderson, E. P., and Brockman, R. W. (1964) Feedback inhibition of uridine kinase by cytidine triphosphate and uridine triphosphate. *Biochim. Biophys. Acta* 91, 380–386.
- (5) Plagemann, P. G., Ward, G. A., Mahy, B. W., and Korbecki, M. (1969) Relationship between uridine kinase activity and rate of incorporation of uridine into acid-soluble pool and into RNA during growth cycle of rat hepatoma cells. *J. Cell. Physiol.* 73, 233–249.
- (6) Sköld, O. (1960) Enzymes of uracil metabolism in tissues with different growth characteristics. *Biochim. Biophys. Acta* 44, 1–12.
- (7) Hansen, T., Arnfors, L., Ladenstein, R., and Schönheit, P. (2007) The phosphofructokinase-B (MJ0406) from *Methanocaldococcus jannaschii* represents a nucleoside kinase with a broad substrate specificity. *Extremophiles* 11, 105–114.
- (8) Hazra, S., Sabini, E., Ort, S., Konrad, M., and Lavie, A. (2009) Extending thymidine kinase activity to the catalytic repertoire of human deoxycytidine kinase. *Biochemistry* 48, 1256–1263.
- (9) Iyidogan, P., and Lutz, S. (2008) Systematic exploration of active site mutations on human deoxycytidine kinase substrate specificity. *Biochemistry* 47, 4711–4720.
- (10) Knecht, W., Sandrini, M., Johansson, K., Eklund, H., Munch-Petersen, B., and Piskur, J. (2002) A few amino acid substitutions can convert deoxyribonucleoside kinase specificity from pyrimidines to purines. *EMBO J.* 21, 1873–1880.
- (11) Yokoyama, S., Hirota, H., Kigawa, T., Yabuki, T., Shirouzu, M., Terada, T., Ito, Y., Matsuo, Y., Kuroda, Y., Nishimura, Y., Kyogoku, Y.,

Miki, K., Masui, R., and Kuramitsu, S. (2000) Structural genomics projects in Japan. *Nat. Struct. Biol.* 7, 943–945.

(12) Suzuki, N. N., Koizumi, K., Fukushima, M., Matsuda, A., and Inagaki, F. (2004) Structural basis for the specificity, catalysis, and regulation of human uridine-cytidine kinase. *Structure* 12, 751–764.

(13) Appleby, T., Larson, G., Cheney, I., Walker, H., Wu, J., Zhong, W., Hong, Z., and Yao, N. (2005) Structure of human uridine-cytidine kinase 2 determined by SIRAS using a rotating-anode X-ray generator and a single samarium derivative. *Acta Crystallogr. Sect. D Biol. Crystallogr.* 61, 278–284.

(14) Kuramitsu, S., Hiromi, K., Hayashi, H., Morino, Y., and Kagamiyama, H. (1990) Pre-steady-state kinetics of *Escherichia coli* aspartate aminotransferase catalyzed reactions and thermodynamic aspects of its substrate specificity. *Biochemistry* 29, 5469–5476.

(15) Di Pierro, D., Tavazzi, B., Perno, C. F., Bartolini, M., Balestra, E., Calò, R., Giardina, B., and Lazzarino, G. (1995) An ion-pairing high-performance liquid chromatographic method for the direct simultaneous determination of nucleotides, deoxynucleotides, nicotinic coenzymes, oxypurines, nucleosides, and bases in perchloric acid cell extracts. *Anal. Biochem.* 231, 407–412.

(16) Agarwal, K. C., Miech, R. P., and Parks, R. E., Jr. (1978) Guanylate kinases from human erythrocytes, hog brain, and rat liver. *Methods Enzymol.* 51, 483–490.

(17) Iino, H., Naitow, H., Nakamura, Y., Nakagawa, N., Agari, Y., Kanagawa, M., Ebihara, A., Shinkai, A., Sugahara, M., Miyano, M., Kamiya, N., Yokoyama, S., Hirotsu, K., and Kuramitsu, S. (2008) Crystallization screening test for the whole-cell project on *Thermus thermophilus* HB8. *Acta Crystallogr. Sect. F Struct. Biol. Cryst. Commun.* 64, 487–491.

(18) Ueno, G., Kanda, H., Hirose, R., Ida, K., Kumasaka, T., and Yamamoto, M. (2006) RIKEN structural genomics beamlines at the SPring-8; high throughput protein crystallography with automated beamline operation. *J. Struct. Funct. Genomics* 7, 15–22.

(19) Otwinowski, Z., and Minor, W. (1997) Processing of X-ray diffraction data collected in oscillation mode. *Methods Enzymol.* 276, 307–326.

(20) Vagin, A., and Teplyakov, A. (1997) MOLREP: An Automated Program for Molecular Replacement. *J. Appl. Crystallogr.* 30, 1022–1025.

(21) McRee, D. E. (1992) A visual protein crystallographic software system for X11/Xview. *J. Mol. Graph.* 10, 44–46.

(22) Brünger, A. T., Adams, P. D., Clore, G. M., DeLano, W. L., Gros, P., Grosse-Kunstleve, R. W., Jiang, J. S., Kuszewski, J., Nilges, M., Pannu, N. S., Read, R. J., Rice, L. M., Simonson, T., and Warren, G. L. (1998) Crystallography & NMR system: A new software suite for macromolecular structure determination. *Acta Crystallogr. Sect. D Biol. Crystallogr.* 54, 905–921.

(23) Laskowski, R. A., MacArthur, M. W., Moss, D. S., and Thornton, J. M. (1993) PROCHECK: A program to check the stereochemical quality of protein structures. *J. Appl. Crystallogr.* 26, 283–291.

(24) Iwai, T., Kuramitsu, S., and Masui, R. (2004) The Nudix hydrolase Ndx1 from *Thermus thermophilus* HB8 is a diadenosine hexaphosphate hydrolase with a novel activity. *J. Biol. Chem.* 279, 21732–21739.

(25) Valentin-Hansen, P. (1978) Uridine-cytidine kinase from *Escherichia coli*. *Methods Enzymol.* 51, 308–314.

(26) Liacouras, A. S., Garvey, T. Q., III, Millar, and Anderson, F. K. E. P. (1975) Uridine cytidine kinase. Kinetic studies and reaction mechanism. *Arch. Biochem. Biophys.* 168, 74–80.

(27) Kondo, N., Nishikubo, T., Wakamatsu, T., Ishikawa, H., Nakagawa, N., Kuramitsu, S., and Masui, R. (2008) Insights into different dependence of dNTP triphosphohydrolase on metal ion species from intracellular ion concentrations in *Thermus thermophilus*. *Extremophiles* 12, 217–223.

(28) Van Rompay, A. R., Norda, A., Lindén, K., Johansson, M., and Karlsson, A. (2001) Phosphorylation of uridine and cytidine nucleoside analogs by two human uridine-cytidine kinases. *Mol. Pharmacol.* 59, 1181–1186.

(29) Cleland, W. W. (1963) The kinetics of enzyme-catalyzed reactions with two or more substrates or products. I. Nomenclature and rate equations. *Biochim. Biophys. Acta* 67, 104–137.

- (30) Deng, Q., and Ives, D. H. (1975) Non allosteric regulation of the uridine kinase from seeds of *Zea mays*. *Biochim. Biophys. Acta* 377, 84–94.
- (31) Blank, J. G., and Hoffee, P. A. (1975) Purification and properties of thymidine phosphorylase from *Salmonella typhimurium*. *Arch. Biochem. Biophys.* 168, 259–265.
- (32) Desgranges, C., Razaka, G., Raboud, M., and Bricaud, H. (1981) Catabolism of thymidine in human blood platelets. Purification and properties of thymidine phosphorylase. *Biochim. Biophys. Acta* 654, 211–218.
- (33) Ooga, T., Ohashi, Y., Kuramitsu, S., Koyama, Y., Tomita, M., Soga, T., and Masui, R. (2009) Degradation of ppGpp by nudix pyrophosphatase modulates the transition of growth phase in the bacterium *Thermus thermophilus*. *J. Biol. Chem.* 284, 15549–15556.